Cobalt doped SnO_2: A new material for thermoelectric application

P.P.Pradyumnan*, Anju Paulson, Muhammed Sabeer N.A

Department of Physics, University of Calicut, Malapuram-673635 , Kerala , India.

DOI: 10.5185/amp.2018/660
www.vbripress.com/amp

Abstract

Due to the environmental crisis of energy, the depletion and increasing price of fossil fuel resources, current research focuses on sustainable and renewable energy sources for power generation. Meanwhile, electricity remains the most convenient form of energy in the near future, the conversion of heat into electricity acquires wide acceptance. Thermoelectric generation can be considered as an amble method to scavenge the heat energy for the generation of electricity. In this work we investigate the structural, chemical and thermoelectric property of SnO_2 based samples with varying concentration of cobalt ion. The thermoelectric properties were measured in a temperature 100-700 ^{0}C and found that cobalt doped samples posses a remarkable effect on transport properties compared to pristine SnO_2. Negative thermopower ensured that electrons are the majority charge carriers. Seebeck coefficient for 5 wt % of cobalt doping was found to be -364 μV/K, so that it can be considered as a potential candidate for thermoelectric application. The figure of merit (ZT) of the material gets enhanced on cobalt doping and found to increase with increment in temperature so that it can be used for high temperature thermoelectric application.

Keywords: Thermoelectricity, seebeck coefficient; thermal conductivity, power factor, figure of merit.

Introduction

With the ever increasing demand for energy and its resources made mankind in the search of new and novel renewable energy materials for power generation. Renewable energy technologies such as solar power, wind power, hydro/thermo power, biomass and biofuel offers promising candidates for sustainable energy and green environment. A thermoelectric material (TE) which belongs to the renewable class of energy source provides a unique solution for power generation by converting thermal energy into electricity with electrons as the working fluid without the requirement of moving components. Thus thermoelectric material opens a new door for energy harvesting and waste heat recovery. The conversion efficiency of a thermoelectric power generator is characterized by a dimensionless parameter figure of merit ZT= $\frac{S^2\sigma}{\kappa_{tot}}T$ where T is the temperature, S is the Seebeck coefficient or thermopower, σ is the electrical conductivity and κ_{tot} is the total thermal conductivity. The term $S^2\sigma$ referred as power factor determines the thermoelectric power generation of the TE material [1, 17].

TE materials found novel applications in power generation include biothermal batteries to power heart pacemakers, deep space applications of NASA's voyager and spacecraft missions using radioisotope thermoelectric generators (RTGs) where solar energy is insufficient to power the control, data collection and communication system [2]. TE refrigeration applications include seat coolers for comfort, localized cooling in computers, infrared detectors, electronic and optoelectronic solid state devices for enhanced working performance. Industrial and Military field demand TE materials to posses higher performance at high temperature compared to conventional TE materials which are unstable and highly toxic. Terasaki et al. report single crystal $NaCoO_4$ posses a high power factor compared to Bi_2Te_3 at 300 K and showed that ceramic oxides have potential application as TE material due to its high thermal and chemical stability and more over they cause less environmental impact [3].

Among oxide semiconductors SnO_2 has attracted a great interest as thermoelectric material for power generation due to its simultaneous high electrical conductivity and optical transparency in the visible region of the electromagnetic spectrum [4]. SnO_2 is an n type semiconductor with a wide band gap of 3.6 eV to 4.3 eV due to the presence of intrinsic defects like oxygen vacancies. Recently, Mohagheghi et al. [5] and S. Yanagiya et al. [6] reported SnO_2 based bulk ceramics as a great potential candidate for n-type elements for thermoelectric power generation at high temperature. For the study of thermoelectric properties of SnO_2 Morgan and Wright measured the Seebeck effect in SnO_2 single crystal and found in the range 50 μV/K to 220μV/K depending on the temperature and concentration of conduction electrons in the sample[7]. Introducing magnetic dopants like Co, Ni in to SnO_2 base material results for the emergence of magnetic properties which can be utilized in nuclear reactors as radioisotope

thermoelectric generator (RTG) [8, 9]. The magnetic dopants will remain magnetically active and there by the variation in thermoelectric properties can be determined. Cobalt oxides are of particular interest as TE material because of its large Seebeck coefficient and semiconducting or metallic electric conductivity [10, 11]. The introduction of massive cobalt ions in SnO_2 lattice will reduce the thermal conductivity and expected to possess an increment in figure of merit [12, 13].

In this contribution we mainly focused on optimizing the transport property by properly tuning the doping concentration of Co ion in SnO_2 matrix for high temperature thermoelectric application.

Experimental

Materials/ Chemicals details

SnO (Sigma Aldrich-99%), CoO (Sigma Aldrich-99%) and ethylene glycol were considered to be the initial constituent in this reaction mechanism.

Material synthesis / Reactions

All the samples belonging to the $Sn_{1-x}Co_xO_2$ series were prepared by standard solid state reaction route. Stoichiometric amount of reactants were mixed in nominal composition with x value varying from 1 to 5 wt % to obtain a homogeneous mixture. Uniform heat transfer can be achieved by the addition of ethylene glycol. The powdered slurry were calcined at 500 ^{0} C for 2 hours to remove the volatile impurities. The resultant powder was compacted into disc shape pellets of diameter 10mm with 3mm thickness and placed for sintering at 900^{0}C for 2 hours.

Characterizations / Device fabrications / Response measurements

The structural characterization was performed at room temperature using Rigaku Miniflex 600 X-ray powder diffractometer (XRD) having CuKα radiation with wavelength λ=1.54 Å. The morphology and chemical compositions of the prepared samples were analyzed using FEG Zeiss Supra 55 scanning electron microscope combined with EDAX measurement. SEM measurements were carried out by coating the sample with gold and palladium in a vacuum chamber at low pressure. Thermoelectric transport properties were investigated as a function of temperature ranges from 300 ^{0} C-700 ^{0} C in a helium atmosphere using ULVAC ZEM-3 M8 which can be able to measure simultaneously both the Seebeck coefficient and resistivity of the samples. The thermal conductivity of the material was measured by a steady state method using rectangular bar shaped pellets (10x3x1 mm^3) made under high pressure in an inert atmosphere. The temperature gradient is maintained in the sample and the temperature is recorded using the standard copper-constantan thermocouple.

Results and discussion

The XRD pattern corresponding to the varying composition of $Sn_{1-x}Co_xO_2$ was shown in **Fig. 1**. The XRD confirms the tetragonal structure of SnO_2 with P42/mnm space group. The peaks are indexed and found to be in good agreement with the ICDD data (PDF# 01-070-6995) which confirms the single phase poly crystalline pure structure of the synthesized material. The particle size of the prepared sample was determined using Scherrer equation and it falls in the range 25.7-34.8 nm. Introduction of cobalt ion decrease the particle size, which shows the reduction in grain growth and on further increase in cobalt doping, particle size increases and are found to be less than the pure SnO_2.Based on the radii of Co^{3+} (0.68 Å), Co^{2+} (0.79Å) and Sn^{4+}(0.83Å), the crystal lattice is expected to contract with Co doping [14]. The cell parameters a and c decrease with cobalt concentration which results for the decrement in cell volume. The shift in lattice planes to higher 2θ with increase in cobalt concentration ensures the lattice contraction with doping. Reduction in the intensity pattern can be explained on the basis of low atomic scattering factor for the cobalt ions. The atomic scattering factor for the cobalt (Z=27) is almost half compared to Sn atom. Variation in particle size and cell volume with an increase in cobalt concentration was given in **Table 1**.

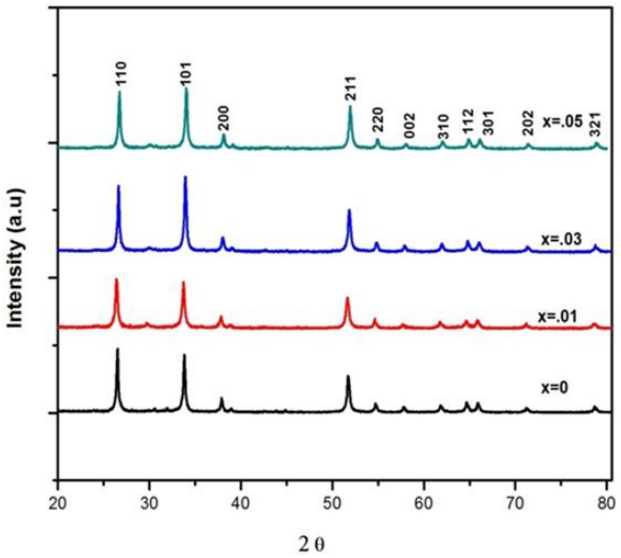

Fig. 1. Room temperature XRD pattern of pure SnO_2 and that of the doped samples.

Table 1. Variation of particle size and cell volume with increase in cobalt concentration.

Wt % of Cobalt	Average particle size (nm)	Cell volume (Å^3)
0	34.75	71.61
1	25.69	70.51
3	32.64	70.19
5	32.78	68.39

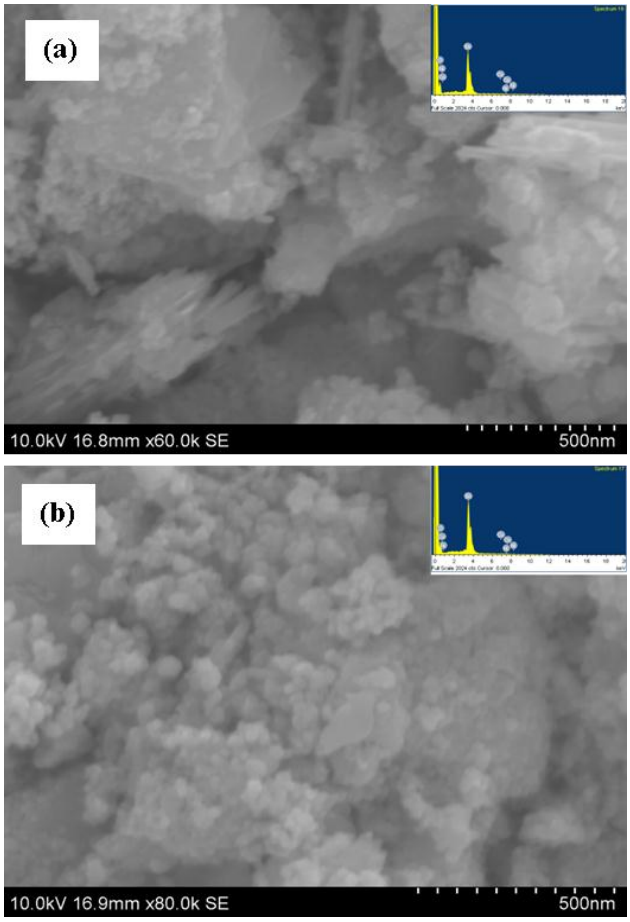

Fig. 2. SEM and EDAX of (a) Pure SnO_2 (b) $Sn_{0.95}Co_{0.05}O_2$

The surface morphology of the samples was studied using scanning electron microscopy (SEM). Significant variation in morphological properties with cobalt doping was observed. The SEM image clearly depicts the incorporation of cobalt ion in the SnO_2 host lattice and thereby cause a reduction in particle size which lies in the range 25-65 nm. Reduction in particle size of the cobalt doped samples due to its accumulation at the grain boundary which act as a kinetic barrier for further grain displacement and hinder the grain growth. Due to the accumulation at the grain boundary scattering of phonons will be prominent and thereby cause a reduction in thermal conductivity. Chemical composition of the samples was ensured using EDAX analysis.

The variation of Seebeck coefficient with doping concentration and temperature ranging from 300^0C-700^0C for pure and cobalt doped samples were shown in **Fig. 3.** As the temperature increases the Seebeck coefficient or thermopower of the material increases due to the increment in the number of charge carriers which overcome the fermi energy level. As the temperature increases above the energy for intrinsic excitation, the Seebeck coefficient begins to decrease due to cancellation of the thermoelectric voltage by holes and electrons during the course of thermal excitation [15]. The negative value for the Seebeck coefficient depicts that the majority charge carriers are electrons. Increase in cobalt ion concentration in pristine SnO_2 increase the induced voltage developed within the material. Since Co^{2+} ion act as an acceptor in SnO_2 lattice it will generate an acceptor energy level near the valence band. Electrons will move from the valence band to the acceptor energy level with creation of holes in the valence band which are responsible for the induced emf generated. When the concentration of cobalt ion increase, much more electrons will leave the valence band and thereby increase the induced thermoemf. The Seebeck coefficient has been obtained as high as -364 µV/K at 748 K, for 5 weight percentage of cobalt doping.

Conductivity measurement of cobalt doped SnO_2 corresponding to the maximum Seebeck coefficient is shown in the **Fig. 4** for the temperature range 300^0C - 700^0C. As the temperature increases the electrical conductivity increases, which shows the semiconducting behavior of the measured samples. The substitution of cobalt into the host matrix should not bring much drastic change to the conductivity compared to pure SnO_2. Introduction of acceptor impurities will generate holes that will combine with free electrons in the SnO_2 host lattice and thereby suppress the electrical conductivity of the doped samples. With increase in doping concentration the holes become the majority charge carriers and we expect a gradual increase in the electrical conductivity. Mass fluctuation introduced by the lattice point substitution will scatter electrons and thereby reduce the electrical conductivity.

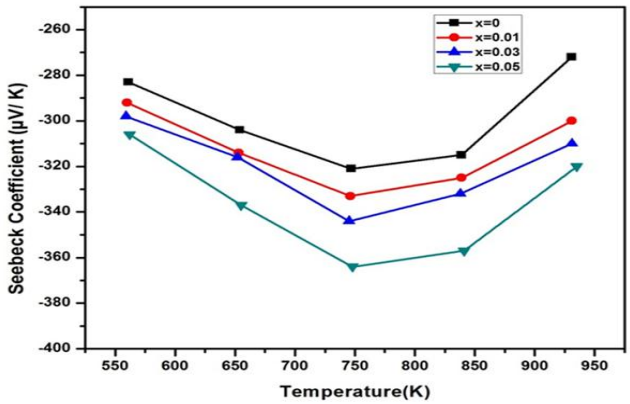

Fig. 3. Variation of Seebeck coefficient with doping concentration.

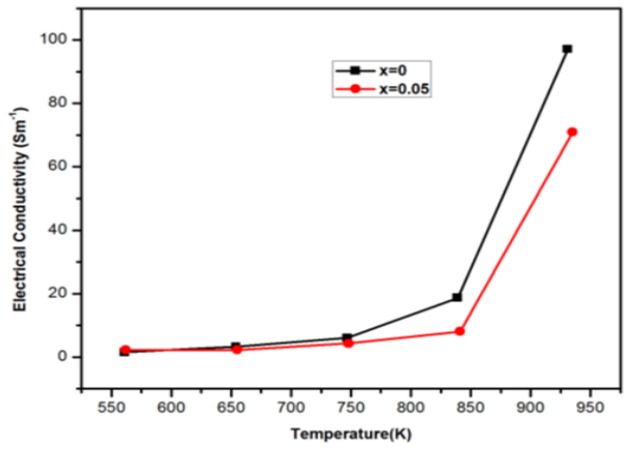

Fig. 4. Variation of electrical conductivity with temperature.

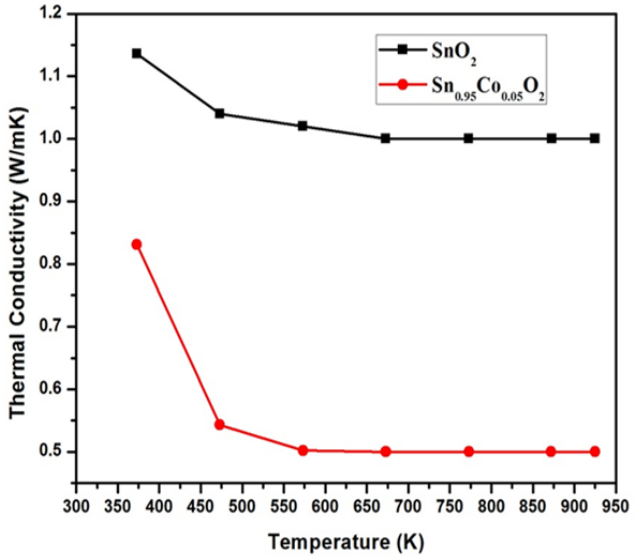

Fig. 5. Variation of thermal conductivity with temperature.

The thermal conductivity of the samples was shown in **Fig. 5** for the temperature range 300-900 K. The total thermal conductivity can be expressed as $\kappa_{tot} = \kappa_e + \kappa_L$; where κ_L and κ_e is the thermal conductivity due to lattice phonons and electrons respectively. Thermal conductivity due to electrons can be determined by Wiedemann Franz law $\kappa_e = LT\sigma$, where σ is the electrical conductivity, T refers to temperature and the constant defined as Lorentz number $L = 2.45 * 10^{-8}\ V^2\ K^{-2}$. κ_e has a low contribution to the total thermal conductivity in the measured temperature range and accordingly κ_L is the predominant component in κ_{tot} and the variation mainly arises from the alteration in κ_L. As the temperature increases the scattering of phonons at the grain boundary increases and thereby cause a reduction in heat transfer. Scattering mechanism arises due to the presence of impurities, grain boundaries or phonons in the lattice site. The substitution of cobalt in the host lattice will introduce a lattice disharmony and strongly scatter the phonons and thereby cause a reduction in thermal conductivity. At low temperature the main scattering mechanism occurs due to the presence of impurity ions and grain boundaries,whereas at high temperature scattering due to phonons will be more prominent termed to be the umklapp scattering and found to be independent of temperature.

Fig. 6 shows the calculated dimensionless figure of merit ZT as a function of temperature corresponding to pure and 5 wt % cobalt doped sample. For both the samples ZT monotonously increases as temperature rises. The figure of merit is strongly enhanced by Co addition at 925 K. There occurs a 50 % increase in ZT value with cobalt incorporation at 750 K. This is attributed to the increase in thermopower and reduction of thermal conductivity due to the substitution of cobalt with Sn.

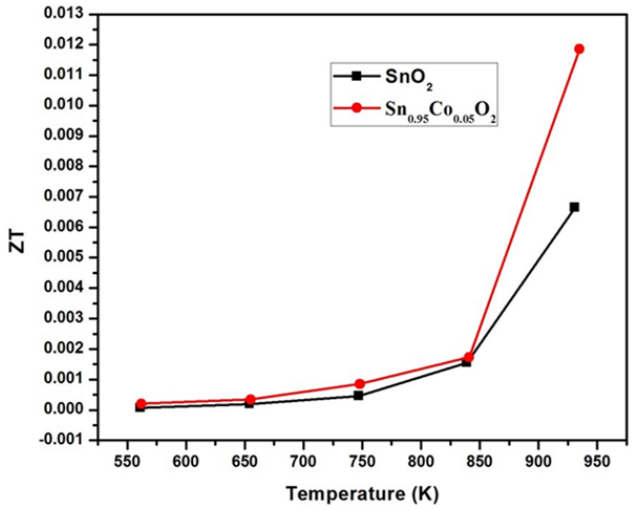

Fig. 6. Temperature dependence of figure of merit.

Conclusion

Pure and cobalt doped SnO_2 compounds were synthesized by solid state reaction by varying the concentration of the dopants from 0 to 5 weight %. XRD analysis revealed the phase purity of the synthesized material and particle size found to decrease with increase in doping concentration. Surface morphology of the compounds was analyzed using Scanning Electron Microscope and substantiate the reduction in particle size. EDAX spectrum proves the incorporation of cobalt in the host SnO_2 lattice. No trace of other elements in the spectrum ensures the purity of the samples. Measurement of thermoelectric properties revealed that Cobalt doped SnO_2 can be considered as a good candidate for thermoelectric application owing to its increase in thermopower and reduction in thermal conductivity. The thermoelectric performance of the material is determined for the ZT value and it increase with temperature and found to be much greater for the cobalt doped samples. Thus Cobalt doped SnO_2 can be considered as a good candidate for high temperature thermoelectric application.

Acknowledgements

The author PPP is thankful to DST SERB, Govt of India for financial assistance in the form of major research project entitled "Studies on oxide materials for thermoelectric generation " (No.SB/EMEQ 002/2013 dated 5/7/2013). The authors also thankful to DST Govt of India for financial support through FIST programe (SR/FIST/PS1-159/2010) and UGC Govt of India SAP programe F 530/2/DRS/2013(SAP-I), Department of Physics ,University of Calicut.

Author's contributions

Conceived the plan: PPP,AP; Performed the experiments: NAMS,AP; Data analysis: PPP,AP,NAMS; Wrote the paper: PPP,AP,NAMS

References

(a) Scientific article

1. Jeffery W. Fergus; J. Eur. Ceram. Soc., **2012**, 32, 525-540.
2. Koumoto, K.; Teraski, I.; Funahashi, R.; *MRS Bull*, **2006**, 31, 188-198.

3. Terasaki,I; Y. Sasago; K. Uchinokura; Phys. Rev. B,**1997,** 56.
4. Fahrettin Yakuphanoglu; *J.Alloys Compd*, **2009**, 470, 55-59.
5. Mohammad-Mehdi Bagheri-Mohagheghi ; Mehrdad Shokooh-Saremi; Phys. B**, 2010**, 405 , 4205–4210.
6. S. Yanagiya,; N.V. Nong; J. Xu; M. Sonne; N. Pryds ;J. Electron. Mater. **2011,**40,674.
7. D.F. Morgan; D.A. Wright; Br. J. Appl. Phys, **1996**, 17, 337.
8. Bérardan,D.; Guilmeau,E;, Maignan, A.; Bernard Raveau ; *Solid State Commun*,, **2008**, 146, 97–101.
9. Park K; Seong JK, Kim GH; *J.Alloys Compd;* **2009**, 473, 423–427.
10. Z.Q. Li, J.J. Lin; *J. Appl. Phys*; **2004**, 96, 5918.
11. Galatsisa, K; Cukrov, L; Wlodarski, W; McCormick, P; Kalantar-zadeh, K; Comini, E; Sberveglieri, G; Sens. Actuators, B, **2003**, 93, 562-565.
12. Antoine Maigna; Sylvie Hebert; Li. Pi, D. Pelloquin, B. Raveau; Cryst. Eng.; **2002**, 5,365-382.
13. Yanfeng Zhang; Jiuxing Zhang; Qingmei Lu; Ceram. Int.; **2007**, 7, 1305-1308.
14. T. Ramachandran; N. E. Rajeevan; P. P. Pradyumnan; Mater. Sci. Appl., **2013**, 4, 816-821.
15. Francis. J. DiSalvo; *Science*, **1999**, 285, 703-706.
16. Yong Liu; Wei Xu; Da-Bo Liu; Meijuan Yu; Yuan-Hua Lin; Ce-Wen Nan; Phys. Chem. Chem. Phys., **2015**,17, 11229-11233.

(b) Book

17. Tiwari, A.; Kobayashi, H. (Eds.); Responsive Materials and Methods; Wiley: USA, **2013**. D.M Rowe (Ed); Thermoelectric Handbooks Macro to Nano; CRC: Raton, **2006**

